*J Mater Sci* (2019) 54:11357–11377

Review

# Interface formation and bonding mechanisms of hot-rolled stainless steel clad plate

B. X. Liu[1,*], Q. An[1], F. X. Yin[1,*], S. Wang[1], and C. X. Chen[1]

[1] *Research Institute for Energy Equipment Materials, TianJin Key Laboratory of Materials Laminating Fabrication and Interfacial Controlling Technology, School of Materials Science and Engineering, Hebei University of Technology, Tianjin 300132, China*

**Received:** 16 November 2018
**Accepted:** 1 April 2019
**Published online:** 5 April 2019



## ABSTRACT

Since the 1980s, vacuum hot rolling has been developed to fabricate the stainless steel clad plates by the Iron and Steel Institute of Japan. Herein, hot rolling is a widely used solid-state bonding process to join the carbon steel substrate and stainless steel cladding. In this paper, we provide a brief overview of the vacuum hot rolling process and effective parameters on the interface characteristics and shear strength of stainless steel clad plate. The effects of surface preparation condition, atmosphere condition, vacuum degree, rolling temperature, rolling reduction ratio, interlayer, heat treatment on the microstructure, interface characteristics and mechanical properties of stainless steel clad plate have been analyzed in detail. It is shown that the interface transition zone is formed due to the carbon diffusion, and the strong interface bonding is attributed to the sufficient alloy elements diffusion of Fe, Cr and Ni. Moreover, the interface shear strength and toughness are also affected by interfacial precipitation phase and multiple oxides. Finally, the present work concluded the bonding mechanism of hot-rolled stainless steel clad based on the oxide film theory, diffusion theory, recrystallization theory and three stage theory.

## Introduction

As a part of large group of laminated metal composites, stainless steel clad plates realizing the possibility of combining the weldability, formability of carbon steel substrate with the high corrosion resistance of stainless steel cladding have been used for several decades [1], which have a number of widespread applications in pressure vessels, heat exchangers, nuclear power equipment, desalination equipment, bridge engineering, hull, automobile, armor, etc. [2–8]. At present, there are mainly three kinds of bonding methods to produce stainless steel clad plates used in the industry [1]: overlayer welding, explosive welding and hot rolling, and the interface microstructure and characteristics are shown in Fig. 1. Herein, overlayer welding can obtain uniform bonding interface and high shear strength between carbon steel and stainless steel; it is mainly used for producing complex parts as well as cladding on unreachable areas. However, the generated energy and thermal stress will deteriorate the interface

Address correspondence to E-mail: liubaoxiliubo@126.com; yinfuxing@hebut.edu.cn

https://doi.org/10.1007/s10853-019-03581-x

microstructure, mechanical properties and corrosion resistance during the overlay welding process as shown in Fig. 1a [9], leading to the microscale cracks formed at the interface [10–13]. Explosive welding takes advantages of very short duration time and high-energy impulse of an explosion to drive two surfaces of metal together, simultaneously cleaning away the oxide film and creating a good condition of metallic bonding, and perfectly clean surfaces and wavy interface can be obtained under pressure and severe plastic deformation as shown in Fig. 1b [13]. However, this method has many shortcomings, such as low production, low product quality, low dimensional accuracy, high contaminant and thermal residual stress. Actually, the thickness of stainless steel cladding cannot be lower than 3 mm due to the huge shock wave and severe wave-like interface. In addition, serious noise pollution and explosive pollution limit the practical production and application of explosive bonding [10–13]. In addition to the above three main methods, there are many other methods to produce stainless steel clad plates, such as laser cladding [14], diffusion welding [15, 16], electromagnetic pulse welding [17], ultrasonic welding [18], etc.

Since the 1980s, the hot rolling method has been developed to fabricate stainless steel clad plates, and there are many reports in research journals published by various institutes, such as the Iron and Steel Institute of Japan and the Japan Welding Society [1, 19–21], and corresponding interface microstructure and characteristics are shown in Fig. 1c [19]. Recently, more than ninety percents of stainless steel clad plates have been produced by vacuum hot rolling, which is attributed to the few interface defects, high efficiency and continuity compared with other above two methods [1, 22–24].

Interface bonding status and shear strength are taken as main factors to evaluate the quality of stainless steel clad plate [25, 26], and the interface shear strength determines the usefulness of laminated metal composites in subsequent forming processes, such as cutting, forging, rolling, bending, joining, deep drawing, stretch forming, etc. [27–36]. Liu et al. reported that strong interface shear strength can delay the premature localized necking, contributing to the superior fracture elongation of laminated metal composites [37–39]. Atrian et al. [36] reported that strong interface shear strength can prevent wrinkling and delamination fracture of metal clad plates during deep drawing and other forming processes. Kum et al. [40] and Liu et al. [38, 41] proposed that the impact energy and bending toughness of laminated metal composites can be enhanced by the weak interface. The process parameters affecting the interface shear strength involve the surface

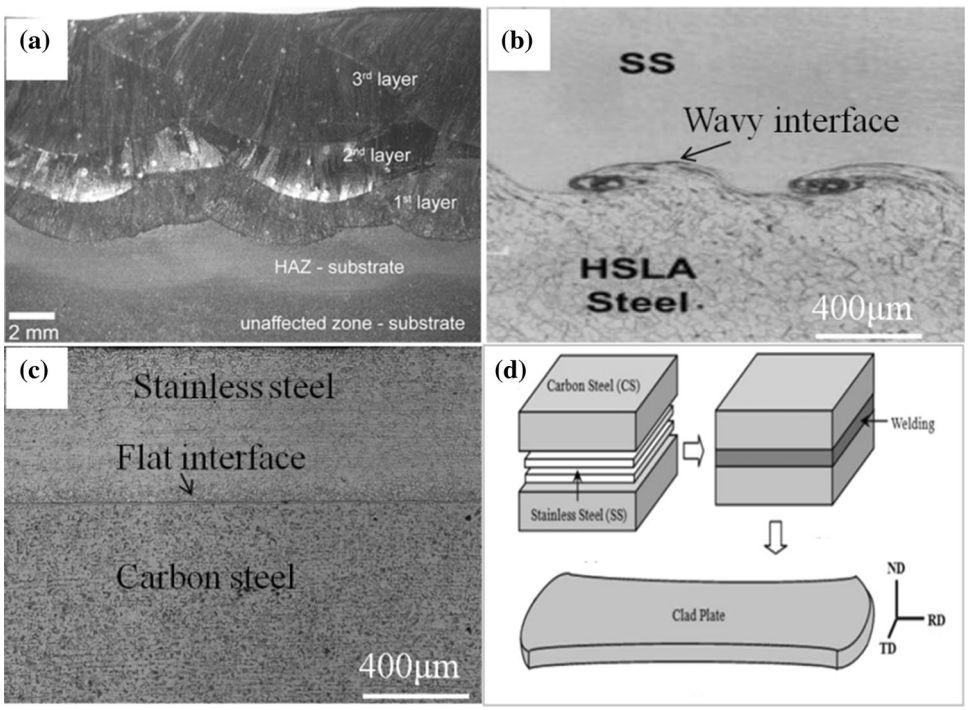


**Figure 1** The interface microstructures of three bonding methods and diagrams illustrating of fabrication process of hot-rolled stainless steel clad plate. **a** Overlayer welding [9]; **b** explosive welding [13]; **c** hot rolling [19]; **d** fabrication process of hot-rolled stainless steel clad plate: surface preparation and assembling, welding and pumping vacuum and hot rolling [2, 4].

preparation and deformation conditions, specimen size, vacuum degree, the number of rolling passes, rolling temperature, rolling reduction ratio, etc. [2, 25, 42].

Vacuum hot-rolled stainless steel clad plates have many shortcomings as follows [24, 43]: (1) Low carbon steel substrate matrix contains annealing ferrite and pearlite microstructure, which always displays low strength compared with the stainless steel cladding. It cannot be fitting to the practical service requirement of stainless steel. (2) Stainless steel cladding always contains deformation defects and sensitized particles, such as strain-induced martensite phase and intergranular $Cr_{23}C_6$ particles, which seriously affect the mechanical properties and corrosion resistance of stainless steel clad plate. (3) Carbon diffusion leads to formation of carburized layer and decarburized layer, which can result in the decrease in corrosion resistance at the clad interface. (4) Low rolling reduction, rolling temperature and low vacuum degree can always result in the weak clad interface, which can also induce the interface delamination. Therefore, vacuum hot rolling process always leads to unstable interface microstructure and properties, which seriously affects the forming and service application of stainless steel clad plates, especially for the thick and wide stainless steel clad plate.

In this article, the effects of process parameters on interface shear strength of stainless steel clad plate, including surface preparation, rolling reduction ratio, vacuum degree, rolling temperature and the number of rolling passes, as well as bonding interface microstructure, interface alloy element diffusion, heat treatment behavior and bonding mechanisms are summarized and analyzed. It is useful to further comprehend the relationship between fabrication parameters and mechanical properties of stainless steel clad plate and provide the design route with low cost and large size to industrially produce stainless steel clad plate with strong interface bonding status.

## Hot rolling

Figure 1d shows the schematic illustration of hot rolling for the production of stainless steel clad plate [2, 4]. In the hot rolling process, the carbon steel substrate and stainless steel cladding are stacked symmetrically [2, 4] or asymmetrically [44, 45] together and then passed through a pair of roll millers until a critical deformation ratio achieved to produce a solid-state bonding between the original individual metal pieces. Before hot rolling process, the surfaces of carbon steel substrate and stainless steel cladding to be bonded should be properly cleaned and prepared to remove the contamination layer, anodized layer and oxide layer. Metal surfaces are covered with grease, chemical compounds, adsorbed moisture oxide film, etc., which can inhibit the interface bonding [25]. Therefore, the metal surfaces before hot rolling play an important role in influencing the interface bonding status. There are many surface preparation processes in hot or cold rolling process, including mechanical, thermal and chemical treatments [46]. Herein, the surfaces of steel plates were mechanically cleaned by wire brush to remove the contamination and oxide layer, which is the best way to prepare a clean metal surface [2].

Then, in order to avoid the oxidation of the bonding interface of stainless steel clad plates, two stainless steel plates were shielded with the high-temperature isolate cloth or particles and then spot-welded to fix together, and the carbon steel plates were symmetrically stacked with stainless steel plates [2, 4]. The inner surfaces of two pieces of carbon steel plates were welded with four carbon steel seals, and a hole was drilled in the middle of one seal. The hole was joined with a stainless steel pipe by tungsten inert gas (TIG) welding, and it was suitable to pump the air out of the interior space of green blanks and make a vacuum environment using a triplex diffusion pump [2]. Finally, the pipe was sealed and welded by hydraulic pressure clamp. During the hot roll bonding process, the high rolling temperature and reduction ratio generated a great amount of heat, plastic deformation and virgin surfaces on the metals being roll bonded [35]. After the above processes, a proper treatment was performed after hot rolling to obtain a combination of high strength, ductility and corrosion resistance [4].

## Parameters affecting bonding interface

Many process parameters relating to the hot roll bonding have been carried out to understand the complex nature of the bonding mechanisms of stainless steel clad plates [2, 4, 44]. It has been concluded that the interface bonding of stainless steel

clad plates is affected by various processing factors, such as rolling reduction ratio [47], rolling temperature [2], surface roughness [48], atmosphere condition [4], interlayer [49], heat treatment [3], etc.

## Surface roughness condition

The interface shear strength is affected by surface roughness condition during the rolling process. It is reported that the polished surface degreased in acetone did not bond, and the maximum interfacial shear strength increases with the increasing friction coefficient caused by surface roughness during the roll bonding process [50]. Moreover, it is shown that at a low rolling reduction ratio and a small coefficient of friction, the interface bonding was not successful. This is because that the mean interface stress increases with the increasing friction coefficient between the carbon steel substrate and stainless steel cladding. Wu et al. [51] reported that the initial bonding was difficult to achieve without successful modification to the surfaces. The metallic bonding was obtained at immediate temperature as long as the surface oxide was eliminated completely in the process of hot rolling.

There exists a close relationship between the surface preparation method and interface shear strength of laminated metal composites. Jamaati et al. [50] reported that an increase in surface roughness can cause the increase in number and size of cracks on the surface layers, providing greater areas of extruded virgin metals to be joined, and then improving the interface shear strength of clad plates. The mechanical treatment of metal surface provides a great number of rough asperities and introduces a severe localized plastic deformation with high shear stress and strain that interrupt the formation of the unavoidable surface oxide layer during the rolling process [52]. Meanwhile, the high roughness resulting from the increased brush wire diameter and the decreased wire length may reduce the critical pressure to initiate interface bonding, which is beneficial to enhancing the interfacial shear strength of clad plates [50].

## Atmosphere condition

In general, hot rolling can achieve complete metallurgical bonding interface at a low rolling reduction ratio and rolling pressure in comparison with cold rolling, which is attributed to the severe plastic deformation and recrystallization of two surfaces at the bonding location [53]. Therefore, stainless steel can be always cladded on the carbon steel by hot rolling method due to the super-high yield strength [44]. Herein, interface oxidation is an adverse factor for the important reliability indicator of interface bonding quality, which can lead to the rapid decrease in interfacial shear strength [54]. Many methods used to avoid to the severe interface oxidation are reported as follows:

### *Hydrogen atmosphere*

Jing et al. [44] reported that the stainless steel clad plates were successfully hot-rolled after reduction descaling in pure hydrogen atmosphere. The oxide scale on the surfaces of two individual steels was perfectly depleted when the reduction time was above 10 min at 900 °C. Many tiny cracks existed on the surfaces of carbon steel and stainless steel, which are attributed to oxidization of metallic surface. However, there were many long lath cracks with the length ranging from several microns to several millimeters and a great number of micropores about 1 μm evenly distributed on the metallic surface after reduction. Subsequently, during the hot rolling process, the quality and dimension of interface cracks and pores were decreased rapidly with the increase in rolling reduction ratio, resulting in the enhanced interfacial shear strength. Moreover, the absence of interface pores and superior interface shear strength of 375 MPa were obtained with the accumulative rolling reduction ratio of 74.5%.

### *Ar atmosphere*

In 2014, Jing et al. [45] found that stainless steel clad plate can obtain good interface bonding status in an argon atmosphere and then be hot-rolled by multiple passes in air. The surfaces of stainless steel and carbon steel are oxidized with a small amount due to the inhibiting of argon gas compared with the air atmosphere environment, and many individual micropores about 3–5 μm can be found along the interface line between the carbon steel substrate and stainless steel cladding in the initial rolling pass. Subsequently, the dimension and percentage of micropores are gradually decreased with the increasing rolling passes, and perfect interfacial bonding is obtained

without any micropores after the fifth rolling pass, which is attributed to the effective and protective environment of Ar atmosphere.

### *Vacuum degree*

Li et al. [49] investigated the interfacial inclusions and shear strength of stainless steel clad plates with different vacuum degrees. It was shown that microstructure, chemical compositions and distribution of interface oxides inclusions can also be related to vacuum degree inside the symmetrical stainless steel billet. Herein, the silicon compounds were dominated at the vacuum degree of 15 Pa or higher and the alumina particles did at the vacuum degree of 0.1 Pa or lower. It is concluded that the presence of interface oxide inclusions may be attributed to the selective oxidation of Al, Si, Mn and Cr elements diffusing from the billet into bonding interfaces between carbon steel substrate and stainless steel cladding [54–56].

Figure 2 shows the typical morphologies of interface oxide inclusions of stainless steel clad plates with different levels of interface oxidation [4]. The interfacial oxides turn from the spheroidal, rod-like shape into the blocky, spheroidal, irregular linear shape. Meanwhile, the length of linear interfacial oxides is gradually increased with the decreasing vacuum degree as shown in Fig. 2a. However, the variation trend of interfacial shear strength of stainless steel clad plate is complex and ambiguous as shown in Fig. 2b. When the vacuum degree is low, interfacial shear strength is declined firstly with the increasing fine interfacial oxide inclusions [4, 54, 56, 57]. But when the size of interface oxides concentrated at the interface area reaches up to a threshold value with farther raising of oxidation level, competitive cracks between decarburized layer and the brittle carburized layer cause the appearance of strength-increasing step. Interfacial tensile shear strength is decreased rapidly along with further oxidation.

Figure 2c shows the alloy element weight percents of clad interface oxides with different vacuum degrees. At a high vacuum degree of 0.01 Pa, aluminum has a high content, while Si and Fe have low contents. The content of Al is gradually decreased, while the contents of Si and Mn are increased with the decrease in vacuum degree. At the vacuum degree of about 100 Pa, the relative contents of Si and Mn reach to maximum values. When the vacuum degree approach to the one bar pressure, the oxidation of Fe element is obvious. Actually, according to the internal oxidation theory, a complex oxidation system is presented at the clad interface during the high-temperature rolling process. Firstly, the Al element has rather strong affinity with O element and always form $Al_2O_3$ whisker. Then the other elements of Si, Mn, Cr, Fe, Ni take part in the oxidation system. According to thermodynamic calculation and Ellingham diagram, the formation of Gibbs free energies of corresponding oxidation system resulting from the above alloy elements at the rolling temperature ranging from 1000 to 1300 °C are shown in Fig. 2d, as well as listed as follows:

$$\Delta G_{Al_2O_3} < \Delta G_{SiO_2} < \Delta G_{MnO} < \Delta G_{Cr_2O_3} < \Delta G_{MnO} < \Delta G_{Fe_3O_4} < \Delta G_{Fe_2O_3} < \Delta G_{NiO}$$

Therefore, at a high vacuum, the Al and Si firstly reacted with O element and form $Al_2O_3$ whisker and $SiO_2$ particles, respectively. At the moderate vacuum degree, Mn and Cr elements react with O element and form MnO and $Cr_2O_3$ particles, respectively. At a low vacuum degree, Fe and Ni elements will react with O element and form $Fe_2O_3$ and NiO particles, respectively. Overall, the different oxides can be obtained by adjusting the vacuum degree during the hot rolling process [4, 54].

## Rolling temperature

In general, hot rolling is a solid-phase joining method under a certain pressure to join same and dissimilar metals at elevated temperature above recrystallization temperature [2, 53]. Compared to cold rolling, hot rolling can reduce the plastic deformation activation energy, as well as obtain complete metallurgical interface bonding at a lower deformation reduction ratio and rolling pressure, which may be attributed to the severe mutual diffusion behavior of alloy element and plastic deformation capacity of the interface zone [58, 59]. Tong et al. [60] and Jin et al. [61] investigated the effect of rolling temperature on the interface bonding mechanism of stainless steel clad plates in two aspects. Firstly, the rolling temperature may influence the interface gap mechanism of rolled clad plate, and the clean metal is easy to squeeze into oxides gap. Secondly, the high rolling temperature induces the interfacial grain recrystallization.

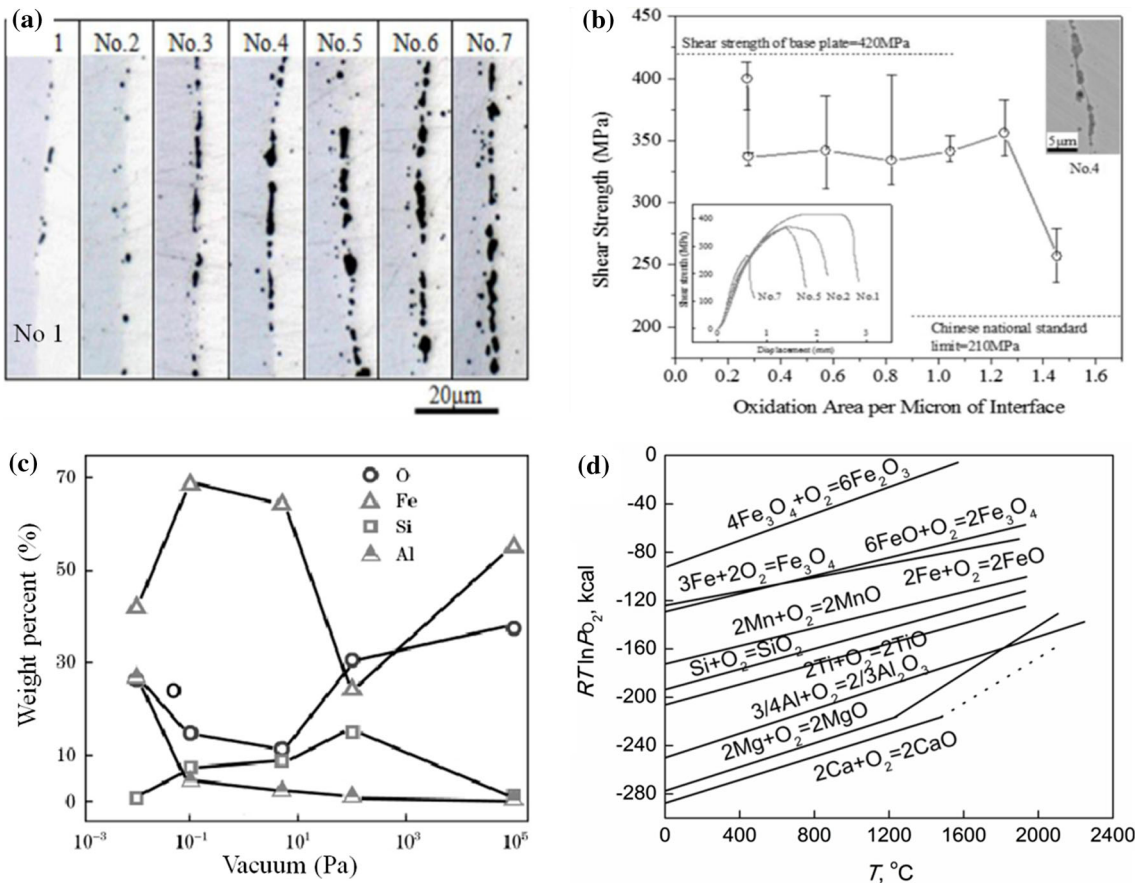


**Figure 2** Interfacial oxides and related mechanical properties, weight percents and $\Delta G_o - T$ relationship of metal oxidation reaction [4, 54]. **a** Interfacial oxides characteristics with different vacuum degrees; **b** relationship between interfacial oxidation and shear strength; **c** weight percent of oxides under various vacuum degree; **d** $\Delta G_o - T$ relationship of metal oxidation reaction.

Liu et al. [2, 25] detailedly described the microstructure, interface characteristics and mechanical properties of stainless steel clad plates fabricated at different rolling temperatures of 1100 °C, 1200 °C and 1300 °C, respectively. The thicknesses of interface reacted zone and the grain size were gradually extended with the increasing rolling temperature. The stainless steel clad plate hot-rolled at 1300 °C obtained the highest fracture elongation and interface shear strength, whereas the lowest tensile strength, which may be attributed to the sufficient alloy element diffusion, matrix recovery and recrystallization at a high rolling temperature. The strong interfacial shear strength can effectively delay the formation of interfacial delamination crack and premature localized necking, resulting into a prolonged uniform plastic deformation stage at a low stress triaxiality. Moreover, the interface shear fractures of stainless steel clad plates rolled at 1100 °C and 1200 °C were located at interface and decarburized layer, respectively. The different fracture characteristics may be related to the sufficient carbon diffusion and interface toughening at a high rolling temperature [4, 22, 26].

## Rolling reduction ratio

Jin et al. [61] proposed that the bonding process of hot-rolled stainless steel clad plates contained three steps: physical contact, activation and diffusion of contact surface, metallurgical bonding. At the physical contact stage, the local contact points of the micro-uneven surface were plastically deformed under the high rolling pressure, and then, the surface contact area gradually expanded, ultimately achieving the entire bonding surface under the continuous pressure. At the second stage, alloy element diffusion, grain boundary migration and chemical reactions have been working on the close contact interface under the high rolling temperature and pressure, and

then, the micropores were vanished, as well as the new reaction phase were formed. Meanwhile, a strong bonding layer was presented at the interface. The third stage was the growth process of metallurgical bonding interface, which is mainly volume diffusion behavior [51, 56, 61, 62].

Xie et al. [22] reported that some obvious strip-like defects indicated as the interstice and Al–Si–Mn–O oxides, and the brittle fracture was appeared at the interface of clad plate at a total rolling reduction ratio of 10%. However, the interstices vanished at the interface, while the ductile fracture occurred in the parent material along transversal direction tensile testing at a total rolling reduction ratio of 70%. Moreover, with the enhancing total rolling reduction ratio, the oxides size was gradually decreased, while transversal direction tensile strength and fracture elongation sharply increased. Tong et al. [60] found that at the high rolling reduction ratio, more cleaner and activated newer interfaces will be obtained and the matrix grain will be refined, contributing higher interface shear strength of stainless steel clad plates [21]. The gradient metallographic changes of grains can also raise the interfacial shear strength of clad plates.

## Heat treatment

The optimal heat treatment condition is necessary to eliminate and decrease the defects during hot rolling process and achieve the structure-function balance between the carbon steel substrate and stainless steel cladding. He et al. [63] reported that roll bonding and subsequent water quenching treatment (920 °C) on stainless steel clad plate can lead to formation of gradient grain distribution at the clad plate, which can obtain superior tensile strength of 1180 MPa and fracture elongation of 8%. Zhang et al. [64] used the off-line induction heat treatment to solution-treated stainless steel clad plate, the result reveals that heat-affected zone of carbon steel substrate contains surface quenching area and intercritical area, and the induction-heated stainless steel clad plate maintains high shear properties. Li et al. [65] reported that Q345R/316 stainless steel clad plate can obtain superior shear strength of 440 MPa by thermo-mechanical control process (TMCP) as follows: rolling at 1000–1200 °C with total reduction ratio of 75% followed by accelerated cooling of 0.2–7 °C/s to below 450 °C and then air cooling. Song et al. [3] reported that the quenching and tempering method employing water quenching after treatment at 1080 °C for 1 h and air cooling after treatment at 550 °C for 1–2 h was more effective than normalized heat treatment, which can enhance the corrosion resistance and mechanical properties of stainless steel clad plate. Tachibana et al. [24] and Liu et al. [43] reported that hot-rolled stainless steel clad plates were successfully strengthened and toughened by quenching treatment at the quenching temperature ranging from 900 to 1150 °C. The clad interface can be effectively strengthened by prolonging the quenching time, and the thickness of carburized layer is decreased with the increasing quenching temperatures ranging from 900 to 1150 °C, short quenching time can't inhibit the formation of interface delamination crack. However, long time quenching treatment leads to sufficient alloy element diffusion at the clad interface, resulting into the strong interface without delamination crack during the tensile testing process.

In conclusion, interface bonding status is mainly related to the interface oxides and alloy element diffusion behavior, and the rolling parameters can affect alloy element diffusion, interface microstructure and interface oxidation. Obviously, the addition of interlayer can inhibit the diffusion behavior of alloy elements, directly resulting into diminution of carburized layer and decarburized layer. The vacuum degree can effectively change the type, distribution, size, shape and number of interface oxides. At a low vacuum degree, interface oxides are relatively coarse, always forming a complete dense interface oxides ceramic wall or film, which are hard to rupture under the condition of high rolling deformation. In this way, the thick interface oxides wall or film can inhibit the alloy element diffusion behavior, leading to weak interface bonding status. However, at a high vacuum degree, the clad interface forms many refined oxides. Meanwhile, the interface oxides are effectively dispersed at the clad interface during the hot rolling process, which can't inhibit the alloy element diffusion behavior. Herein, the clad interface can be strengthened. The rolling temperature can also affect the alloy element diffusion process; Liu et al. have reported that the diffusion distances of alloy element are gradually increased with the increase in rolling temperature [2], which is beneficial to strengthen and toughen clad interface of stainless steel clad plate. Moreover, rolling reduction deformation can make the interface oxides broken and

dispersed along the clad interface, and promote the sufficient diffusion of alloy element. Therefore, the interface shear strength can be improved at high rolling reduction ratio.

## Interface characteristics and fracture behavior

### Interface microstructure and characteristics

The optical interface microstructure of stainless steel clad plate shows that the interface zone mainly contains three zones due to the diffusion of carbon element as shown in Fig. 3 [66–69]: decarburized layer of carbon steel substrate, bonding interface and carburized layer of stainless steel cladding. Herein, the base carbon steel substrate has an 70–90-μm-wide decarburized ferrite layer without pearlite phase adjacent to interface [4], whereas the stainless steel cladding exhibits 30–200-μm-wide carburized layer with poor performance of intergranular corrosion resistance near to the interface as shown in Fig. 3a [2]. The thickness of each layer is related to the rolling temperature, rolling reduction ratio and atmosphere condition etc. [2, 4, 38, 39]. Liu et al. [2] reported that the thickness of decarburized layer remains a constant value, whereas the thickness of carburized layer is increased with the increasing rolling temperature, which may be related to the different diffusion velocity of carbon element in the ferrite phase and austenite phase at the different rolling temperature [26]. Li et al. [47] has illustrated the interfacial microstructure and interfacial alloy element diffusion distribution of hot-rolled stainless steel clad plate as shown in Fig. 3b. Carbon taken as self-interstitial atom has a super-high diffusion velocity in comparison with other alloy elements at a high temperature, which can result in the formation of decarburized layer and carburized layer, respectively. Moreover, it is interesting to note that the concentration phenomenon of C element at the interface, and the C content in the carburized layer is higher than that of decarburized layer, which may be explained in terms of the uphill diffusion effect under the diffusion process [69–71]. It is attributed to the different diffusion velocity and solubility of carbon element in ferrite and austenite, respectively, and the ferrite has high diffusion velocity and low solubility of carbon element compared to the austenite. Therefore, the C atoms are concentrated at the interface. In addition, grain size of decarburized layer is larger than that of the carbon steel substrate. During the cooling process, the pearlite can effectively encourage the nucleation of ferrite in carbon steel. However, the grain of decarburized layer absent of pearlite is hard to refine. Relating to the hardness distribution of stainless steel clad plate, Liu et al. has reported the following conclusions in the previous work [26]: The maximum hardness value is located at the carburized layer due to sufficient solid solution of carbon element, whereas the minimum hardness value is located at the decarburized layer due to the dilution and diffusion of carbon element. Actually, the rolling parameters can't obviously affect the rule of hardness distribution. However, the hardness values can be changed and by selecting different rolling parameters.

In fact, the interfacial bonding status of stainless steel clad plate is mainly related to the diffusion behavior Fe, Cr and Ni elements. In the present work, it is revealed that the diffusion distances of Fe, Cr and Ni are gradually increased, and the interfacial shear

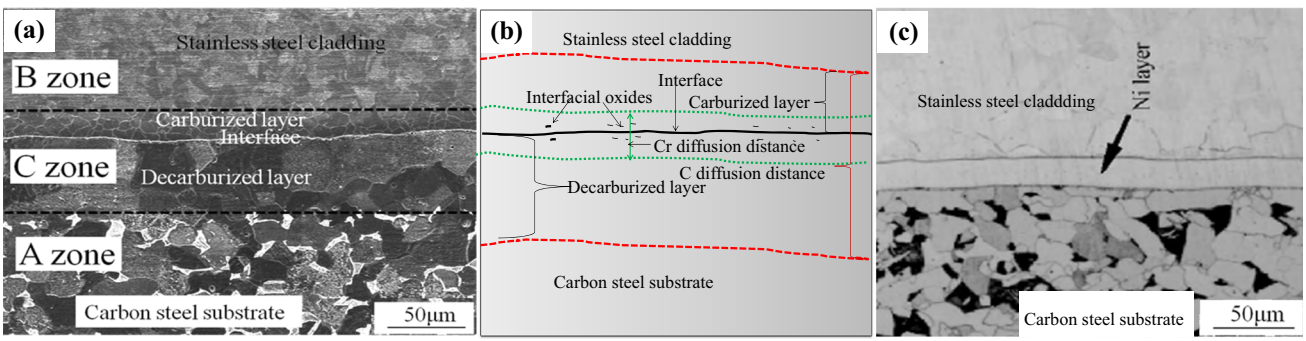


**Figure 3** The microstructure of stainless steel clad plate. **a** Interfacial characteristics and diffusion zones [2]; **b** interfacial alloy element diffusion zones [47]; **c** the addition of Ni interlayer [72].

strength is also increased with the rolling temperature ranging from 1100 to 1300 °C as shown in Fig. 4 [2, 26]. Therefore, the interfacial bonding status is fitting to the diffusion behavior of interfacial alloy elements. Actually, the thicker of the alloy diffusion distance is, the stronger of the interfacial shear strength of clad plates will be [2, 21, 53, 57]. The alloy diffusion at the clad interface belongs to a kind of interfacial metallurgical bonding, which is attributed to the interaction among the atoms of alloy elements. However, excessive diffusion of carbon element may cause the enlargement of weak area including decarburized layer and carburized layer. Therefore, a thick alloy diffusion distance within a certain range can lead to a sufficient metallurgical bonding and the clad interface of stainless steel clad plate can be difficult to be peeled. That is to say, the shear strength of clad plate has been enhanced in some extent. In addition, there are many oxide particles presented at the interface zone. The type, size and morphology of oxide particles are related to the rolling condition and atmosphere condition, which can also affect the interface shear strength and shear toughness of stainless steel clad plates [2, 4].

In order to inhibit the formation of thick decarburized and carburized layer, Li et al. [49, 72] and Xie, Luo and Wang [56, 73] found that the addition of interlayer, such as Ni and Nb interlayers can prevent the diffusion behavior of carbon element. Figure 3c shows that Ni interlayer with 20 μm obviously inhibits the carbon element diffusion behavior, leading to the absence of decarburized and carburized layer. That is to say, the interfacial bonding status and corrosion resistance of stainless steel clad plates can be improved by adding the effective interlayer [72].

## Fracture behavior and mechanisms

### *Shear fracture characteristics*

Figure 5 shows the three shear fracture modes of stainless steel clad plates relating to three different fabrication parameters. The fracture zone of clad plate rolled at 1100 °C is mainly located at the interface as shown in Fig. 5a. It is revealed that the

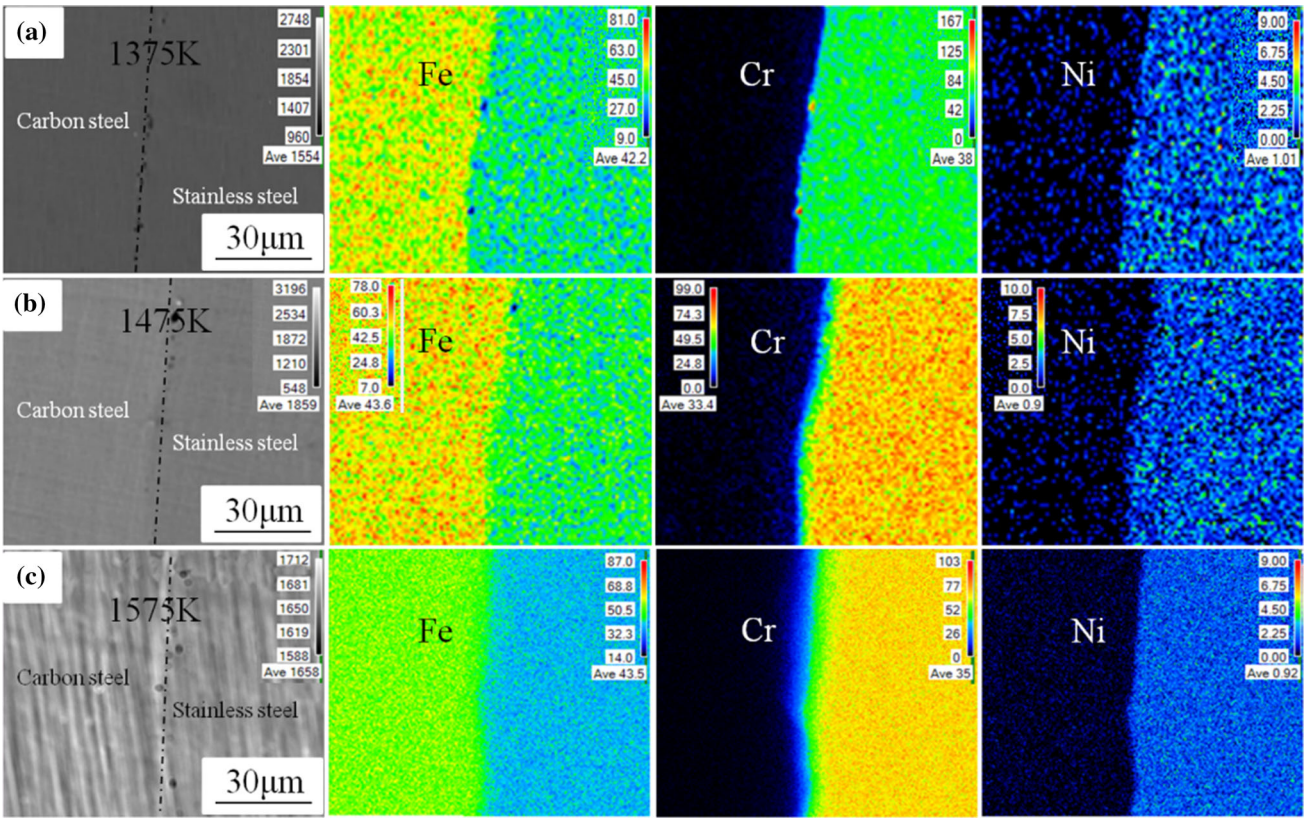


**Figure 4** The interfacial alloying elements EPMA maps of stainless steel clad plates rolled at different temperatures of **a** 1100 °C; **b** 1200 °C; **c** 1300 °C [26].

interface is the weakest position in comparison with decarburized layer, carbon steel substrate and notch position, and the shear strength is the actual shear strength of clad plate. However, the main shear crack of stainless steel clad plate fabricated at 1200 °C is mainly located at the decarburized layer as shown in Fig. 5b. The interfacial bonding status is stronger than that of clad plate at 1100 °C. The decarburized layer has low shear strength and hardness compared to those of the actual interface, which may be attributed to that higher contents of alloying elements are concentrated at the interface, resulting into the relatively strong interface [4, 26]. Figure 5c shows the shear fracture of stainless steel clad plate by adding the Ni interlayer, and it is interesting to note that the main crack is located at the notch position absence of decarburized layer, which reveals that the interface shear strength of clad plate is higher than that of carbon steel substrate.

### *Tensile fracture characteristics*

Figure 6 shows the tensile fracture morphologies of stainless steel clad plates fabricated at different rolling temperatures [2]. Actually, it reveals the fracture behavior relating to the different interfacial shear strength. Firstly, obvious interfacial delamination crack with the length size of 800 μm is presented at the stainless steel clad plate rolled at 1100 °C as shown in Fig. 6a, which may influence the bending loading capacity and further forming behavior to a certain degree. Moreover, deformation incoordination phenomenon can be found between stainless steel cladding and carbon steel substrate at the location of interfacial delamination crack, which is equivalent to the independent deformation of individual layer [2, 74–76]. The carbon steel substrate exhibits a low work hardening rate (n) and uniform plastic deformation capacity compared to the stainless steel cladding. Therefore, the substrate rapidly reaches to the localized necking and then fracture failure [37, 39, 77, 78]. Once the substrate fractures, stress simultaneously concentrates at the stainless steel cladding, resulting into the catastrophic failure of stainless steel cladding and overall clad plate. When the rolling temperature rises to 1200 °C, the interfacial delamination looks nondistinct, and partial interface contains many refined pores and cracks as shown in Fig. 6b. On the whole, the deformation between the substrate and cladding reaches a unanimity and the fracture elongation of clad plate gets a promotion to some extent [2, 27, 30, 79]. Figure 6c shows the profile fracture characteristics of stainless steel clad plate rolled at 1300 °C [2]. Apparently, the stainless steel cladding and carbon steel substrate are considered as a whole, and there are no interfacial delamination and pores during the overall plastic deformation process. That is to say, superior interfacial shear strength is capable to inhibit the formation and propagation of interfacial delamination crack, which can enhance the deformation coordination of stainless steel clad plate. It can also delay the premature localized necking and improve the fracture elongation of stainless steel clad plate to some extent. Meanwhile, strong interface can also improve the loading, plastic deformation and working forming capacity [2, 38, 80, 81]. In addition, there are many intergranular tunnel cracks in the carburized layer

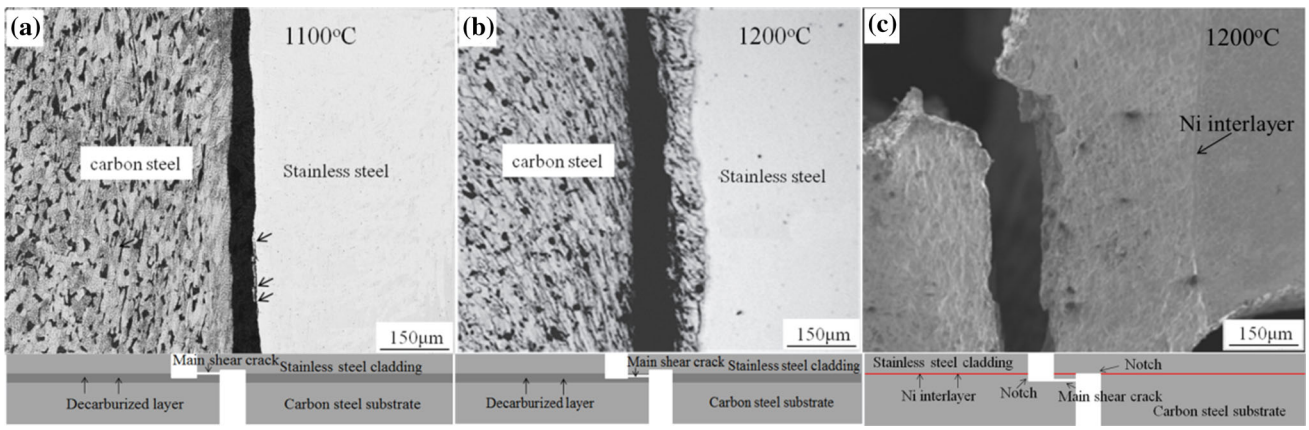


**Figure 5** The shear fracture morphologies of stainless steel clad plates with different rolling temperatures and interlayer. **a** 1100 °C [26]; **b** 1200 °C [26]; **c** the addition of Ni interlayer.

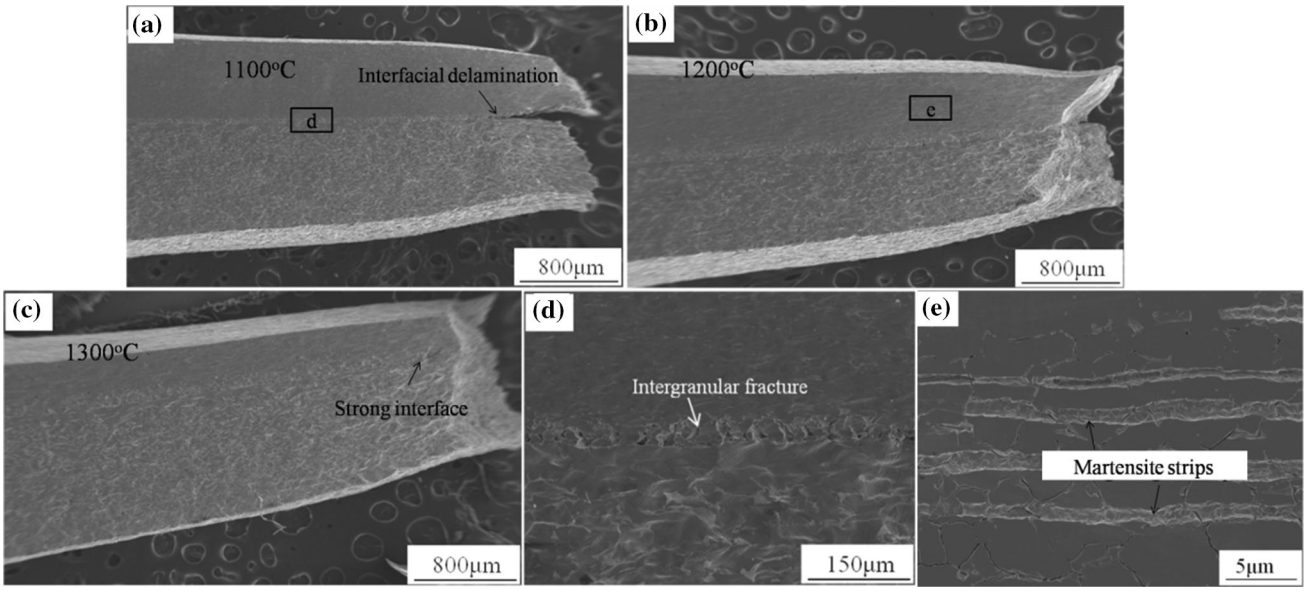


**Figure 6** The tensile fracture morphologies and corresponding characteristics of stainless steel clad plates with different rolling temperatures [2, 26]. **a** 1100 °C; **b** 1200 °C; **c** 1300 °C; **d** intergranular fracture of carburized layer; **e** strain-induced martensite strips.

except the interfacial delamination as shown in Fig. 6d, which give rise to the low fracture toughness and corrosion resistance of carburized layer. Many chromium carbide particles were mounted on the grain boundary in the carburized layer, so that the localized residual stress and even pores are formed at the grain boundary, and the grain interior is lack of Cr element, resulting in the high brittleness, low corrosion resistance and short fatigue lifetime [82, 83]. In addition, many rolling strips are presented in the stainless steel cladding, then the density and thickness of rolling strips are gradually increased with the increase of tensile strain [29, 86,]. Sun et al. [84] reported that the rolling strips may be the martensite phase, and the 304 austenite stainless steel is readily transformed to strain-induced martensite structure by plastic deformation at below $M_d$ temperature [85–87].

## Discussion

### Interface formation and bonding mechanisms

There are many bonding theories about the diffusion welding and roll bonded metallic clad plates as follows: (1) Mechanical occlusal effect, at the initial bonding process, rough surface can induce mechanical occlusal effect of heterologous metals, which can lead to weak interface shear strength during cold rolling process with high reduction ratio [88], while this mechanical occlusal effect is not the dominant factor affecting the hot-rolled clad plate. (2) Metal bond theory, Burton [89] revealed that the surface atoms distance of heterologous metals should reach to the position of mutual attraction between atoms in 1954. Herein, the interface can be bonded due to the atom attraction. (3) Energy theory, Cave and Williams [90] reported that even if the distance of two heterologous atoms reach to the magnitude order of mutual attraction, the interface can't be still bonded if there is no minimum energy for bonding. Only the interface atoms get enough energy to be activated, and the interface bonding status can be obtained. When clean surfaces were mutual contact, there is no interface bonding occurred, revealing that the energy barrier must be overcome before bonding. (4) Diffusion theory, Derby and Wallach proposed [91] that the temperature of interface contact atoms is increased due to the deformation heat, and the interface atoms may be activated and a thin mutual diffusion zone containing solid solution is formed [92], resulting into a great interfacial metallurgical bonding and a strong shear strength. In addition, the diffusion distance can also be seriously affected by chemical potential gradients and diffusion coefficients of various alloy elements. (5) Dislocation theory, this theory reveals that bonding mechanism of

heterologous metals is attributed to the plastic deformation and plastic flow, and the dislocation will migrate to the contact interface when the contact zones of heterologous metals begin to mutual deform coordinately. It results into the fracture failure of interface oxide film and formation of step with a thickness of one atom. More dislocations are generated under the external pressure, leading to increase in plastic deformation resistance and surface roughness. Herein, the interface contact oxide film will break into pieces quickly, which is beneficial to the interface bonding of metallic clad plate [93]. (6) Film theory, this theory reveals that the fracture of surface hardened layer and oxide film can induce the extrusion fresh metal through the cracks, and the interface bonding status can be obtained when the fresh metal surfaces contact and the deformation ratio reaches a critical value to establish contact bonding [25, 94, 95]. (7) Recrystallization theory, Parks [96] thought that the reason of solid–solid interface bonding may be recrystallization, and localized high temperature will enforce the contact interface atoms rearrangement due to high deformation heat. That is to say, a common grain belongs to two heterologous metals is formed, leading to perfect interface bonding status of clad plate [97, 98]. (8) N. Bay theory, Bay [99–102] proposed that bonding mechanism of clad plate contains fracture of work-hardened surface layer, surface expansion increasing the area of virgin surface, extrusion of virgin material through cracks of the original surface layer and establishment of real contact and bonding between virgin material. He implied that normal pressure and surface expansion are basic parameters governing the interface shear strength. (9) Three stages theory, this theory contains three stages: physical contact formation stage, physical and chemical effect stage, "body" interaction stage. At the initial physical contact stage, when the distance of surface atoms between the two heterologous metals reaches to critical distance of mutual attraction and weak chemical bond due to plastic deformation, the dislocations are disappeared, and the surface atoms can be activated and form weak chemical bond. At the physical and chemical effect stages, the activated atoms taken as activated center points are extended to the overall contact surface, and the physical and chemical effect between contact interface results into the strong chemical bond. Finally, at the "body" interaction stage, the mutual diffusion of heterologous metals is carried out by crossing the contact interface, the interface defects are disappeared, and common grains belongs to two heterologous metals are formed, leading to stress relieve and recrystallization [25, 103–105].

Recently, many reports based on transmission electron microscope (TEM) and electron backscattered diffraction (EBSD) investigate the bonding mechanism of metallic clad interface in detail. Pongmorakot et al. [15] reported that the interface shear strength of clad plate is accounted for by the residual compression strain and plastic energy dissipation at the clad interface, and the evolution of interface strength was found to contain two stages: the evolution of first stage primarily takes place in contact interface produced by pressing or rolling pressure, revealing that the disordered atomic arrangement, and the evolution of second stage is attributed to the shrinkage of voids using EBSD and TEM analysis [16].

During the hot rolling process, vacuum degree [4], rolling deformation ratio [106], rolling temperature [2] and the addition of interlayer [72, 73] have significant influences on the interface formation and bonding status of stainless steel clad plate. Actually, the interface formation and bonding mechanism of hot-rolled stainless steel clad plate may be a mixture of above theories, which mainly contains four theories: film theory, diffusion theory, recrystallization theory and three stage theory. Firstly, whatever the atmosphere conditions are, the surfaces of stainless steel and carbon steel are always oxidized to some extent at the high temperature for long holding time, and perfect, partial film or localized oxide particles are formed as shown in Fig. 7a [56]. These oxides may be Mn–Si oxide, $SiO_2$, $Al_2O_3$, even $Fe_2O_3$ during the initial rolling pass [54], and these films or particles will mutually contact and collide with the steel surface, then partial oxide films and particles were broken and squeezed into refined particles, uniformly distributed at the bonding interface [44, 45]. Then the fractured oxide film can induce the extrusion fresh metal through the cracks. Surface grains of clad interface mutually contact and were broken and experience the formation and growth of sintering neck and recrystallization grains [60–62]. Meanwhile, the raw residual pores are gradually closed as shown in Fig. 7b. That is to say, the bonding interface experiences the diffusion process from point, line, face to body types [56]. During the subsequent hot rolling process, the diffusion behavior of alloy

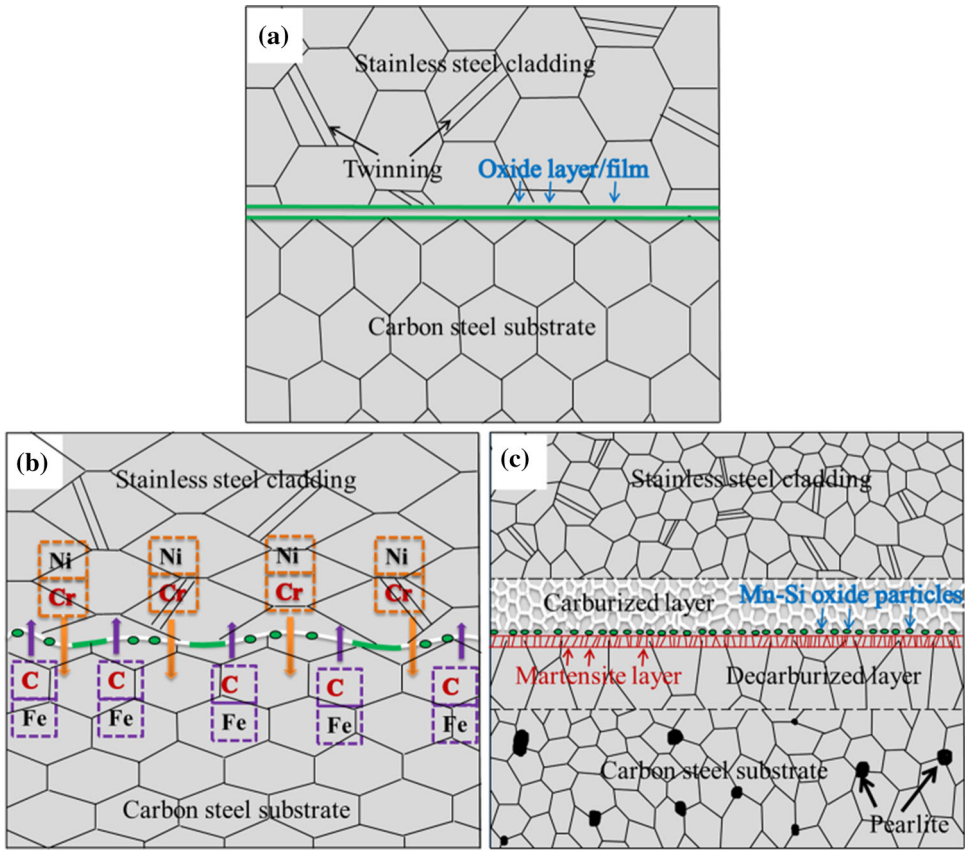


**Figure 7** The interface formation process of stainless steel clad plate. **a** high temperature state; **b** diffusion process and interface formation; **c** interfacial microstructure and characteristics.

elements at the interface is concluded as follows: the C and Fe elements diffuse from the substrate to the cladding, and the Cr and Ni elements diffuse from the cladding to the substrate. Herein, the diffusion zone of carbon and chromium elements can be clearly detected by optical microscopy (OM) and electron probe microanalysis (EPMA), respectively [2, 26]. C diffusion zone contains the decarburized and carburized layer, and the decarburized layer absent of pearlite is taken as a part with weak mechanical properties. It is found that fracture is easy to occur at the decarburized layer under the shear stress condition, and the carburized layer is the worst position with the lowest fracture toughness, corrosion resistance and short fatigue lifetime [107–111].

As for carbon element diffusion, There are mainly two reasons: (1) the high chemical potential gradient of decarburized layer results in the uphill diffusion of carbon element; (2) the carbon diffusion may be related to the different diffusion velocities and solubilities of carbon element in decarburized layer and carburized layer, where ferrite phases and austenite phases exist, respectively. The ferrite has a higher diffusion velocity and a lower solubility of carbon element than austenite. Besides, Liu et al. reported that the decarburized layer has many discontinuously rod-shape carbides [112], which is attributed to the decomposition of lath-like $Fe_3C$. Moreover, the grain boundaries of carburized layer serve as diffusion passage of alloy elements, allowing carbon and chromium atoms to diffuse along grain boundaries and resulting in the precipitation of $Cr_{23}C_6$ at the sensitization temperature range of 420–850 °C. Therefore, the formation of $Cr_{23}C_6$ introduces the depletion of local concentration of chromium element in the grain boundaries, leading to the intergranular corrosion crack of carburized layer. However, Cr and Ni elements are taken as substitutional atoms. The concentration gradients and diffusion coefficients between cladding layer and substrate layer can lead to the diffusion distances of 10–13 μm and 3–4 μm, respectively. The corresponding calculation about diffusion coefficients of Cr and Ni elements is related to Eq. (1).

$$D_i = D_{0i} \exp\left(\frac{Q_{Di}}{RT}\right) \tag{1}$$

where the $R$ (gas constant) and $T$ (environmental temperature) values are 8.314 J/(mol·K) and 1473.15 K. Moreover, the $D_0$ (diffusion constant) and $Q_D$ (diffusion activation energy) values of Cr/Ni elements in γ-Fe are $35 \times 10^{-5}/3.5 \times 10^{-5}$ $m^2/s$ and $2.86 \times 10^5/2.86 \times 10^5$ J/mol. Subsequently, the $D_i$ (diffusion coefficient) of Cr and Ni elements in γ-Fe at the rolling temperature of 1200 °C can be calculated by Eq. (1) to be approximately $2.53 \times 10^{-14}$ and $2.53 \times 10^{-15}$ $m^2/s$. In the similar way, the diffusion coefficients of Cr and Ni elements in α-Fe are $9.89 \times 10^{-13}$ and $1.48 \times 10^{-13}$ $m^2/s$, respectively. Therefore, the higher concentration gradient and ten times higher diffusion coefficient of Cr element than that of Ni element should obtain a thicker diffusion distance. In addition, due to differences in diffusion velocity and concentration gradient of Cr and Ni elements, a certain thin martensite zone is always formed at the clad interface according to Cr and Ni equivalent based on schaeffler diagram as shown in Fig. 7c [56]. The diffusion layer of Cr element represents the actual clad interface, and the clearer the Cr element diffusion is, the thicker of the clad interface and the stronger the interfacial shear strength can be [26]. Therefore, how to inhibit the carbon diffusion and improve Cr diffusion of stainless steel clad plate is the main objective in the future [47]. Wang et al. [56], Xie et al. [73] and Li et al. [72] have reported that the addition of Ni and Nb interlayers can effectively inhibit the diffusion behavior of carbon element, respectively, leading to the decrease in disappearance of decarburized and carburized layers. The interfacial shear fracture is located at the notch of carbon steel substrate, which reveals that interfacial shear strength can be enhanced due to the absence of decarburized layer. Moreover, the surface treatment techniques have attracted more and more attention to strengthen and toughen the steel surface, such as adding TiCN [113, 114], Ti–Cr coatings [115] and ceramic particles (SiCp, $TiO_2$) [116–119] by hot spraying or magnetron sputtering, which are expected to be applied in the field of strengthening and toughening clad interface. Herein, the coatings or ceramic particles don't only inhibit the diffusion behavior of carbon element, but also react with carbon and form the hard particle, being subsequently squeeze into the soft decarburized layer and may effectively enhance the strength and toughness of the decarburized layer.

However, the actual diffusion interface is different from the clad interface fabricated by explosive bonding and overlayer welding [71, 120, 121], and hot-rolled clad interface is straight and uniform, containing many refined ferrite grains with nanometer size, whereas explosive bonded clad interface contains a mount of martensite phases and unbonded regions [122], which result into the decrease of interfacial toughness. The accumulation welded clad interface contains severe residual stress and other metastable structure, such as widmanstatten and martensite phase due to alloying element dilution [121].

## Fracture path and fracture mechanism

In order to explain the tensile fracture behavior of stainless steel clad plate in detail, Fig. 8 illustrates the different crack propagation paths and fracture mechanisms relating to the different interfacial status. When the diffusion distances of Cr and Ni are short, it represents low interfacial vacuum degree, rolling temperature or rolling deformation ratio, so the low interfacial shear strength can be obtained as shown in Fig. 8a. Firstly, intergranular tunnel cracks are formed due to low fracture toughness of grain boundary in the carburized layer [2, 123, 124]. However, the intergranular tunnel cracks can't further propagate and have to accrete due to the prevention of stainless steel cladding and interface as shown in Fig. 8b. With the increase in tensile strain, the interfacial delamination phenomenon is presented due to interfacial misfit and transversal stress, and the carbon steel substrate individually deforms; it is easy to localized necking due to low value of hard-working rate as shown in Fig. 8c [125, 126]. Finally, a catastrophic failure occurs at the carbon steel substrate, and the tensile stress transforms into the carburized layer. The section percent of carburized layer to loading part simultaneously inclined. That is to say, the stress intensity factor at the tunnel crack tip in the carburized layer increases, and the tunnel crack propagates into the stainless steel cladding and results in the fracture failure of overall stainless steel clad plate [127]. Meanwhile, stainless steel cladding form many strain-induced martensite rolling strips as shown in Fig. 8d. Finally, at the stage of fracture failure, more stress-induced martensite phases are formed, and one of tunnel cracks passes through the stainless steel cladding, leading to

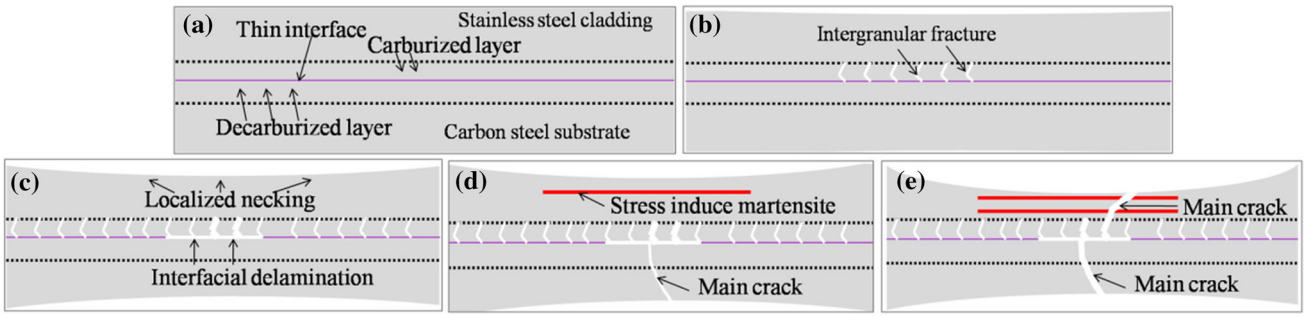


**Figure 8** **a**–**e** The tensile failure process of stainless steel clad plate with weak interface.

fracture failure of overall stainless steel clad plate as shown in Fig. 8e.

Figure 9 shows the fracture paths of stainless steel clad plate with strong interfacial bonding status, which may be related to the high vacuum degree, rolling temperature and deformation ratio. The diffusion distances of Cr, Ni and Fe elements are thick as shown in Fig. 9a. At the early stage of tensile process, intergranular tunnel cracks also experience nucleation, propagation, retention and proliferation processes as shown in Fig. 9b [123]. However, delamination crack is absent at the clad interface due to the strong interfacial shear strength, which delays the premature localized necking and fracture process of carbon steel substrate, improving the deformation coordination of clad plate. At this stage, the proliferation of intergranular tunnel cracks and localized necking of clad plate are mutually competing, and they are playing important roles in toughening clad plate [30, 128–130]. Which one affects the final fracture is decided by the thickness ratio of carburized layer and clad plate, and the final fracture failure is decided by the carbon steel substrate because of the thin carburized layer as shown in Fig. 9c [2]. Finally, microcracks firstly form in the middle of carbon steel substrate, leading to the fracture failure of substrate, and then meet the intergranular tunnel cracks, resulting into the fracture failure of overall clad plate as shown in Fig. 9d [41, 123]. In addition, more severe strain-induced martensite strips remain occurred at the cladding than that of clad plate with low interfacial shear strength, which is attributed to the higher fracture elongation of clad plate [131].

However, if only the pursuit of superior interfacial shear strength, it would result in the decrease of other mechanical properties. Superior bonding status is critical during the tensile, bending, forming and superplastic process, whereas it is not fitting to the impact and fracture toughness of clad plate and multilayer steel [40, 132–137]. In fact, weak interfacial bonding status may induce many partial interfacial delamination cracks, which prolong the crack propagation path and reduce the propagation velocity. Meanwhile, it can also absorb many fracture energy, which is beneficial to enhance impact and fracture toughness [138–141]. Moreover, in the microlaminated or nanolaminated steels, such as TWIP or DP steel, interfacial delamination can also improve the fatigue lifetime [142]. Therefore, single-minded pursuit of superior shear strength often gets backfire conclusion. In addition, super-high rolling temperature, deformation ratio, vacuum degree always form

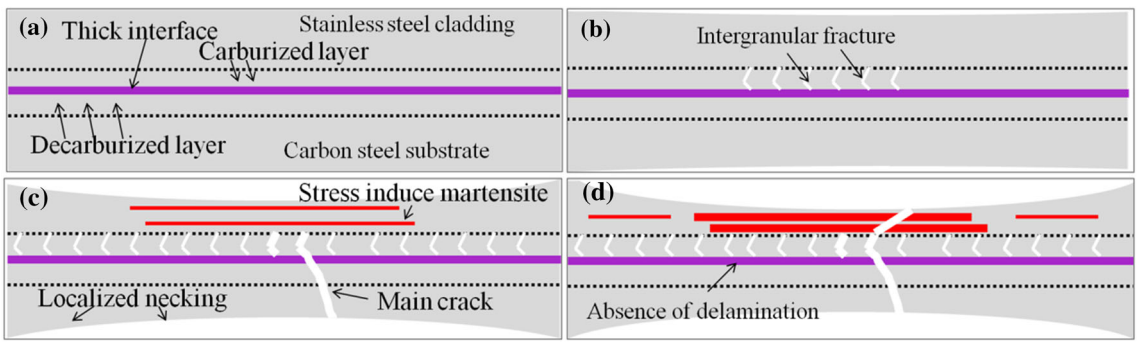


**Figure 9** **a**–**d** The tensile failure process of stainless steel clad plate with strong interface.

severe residual stress and coarse grains at the clad interface, resulting into the decrease in overall mechanical properties [2, 38].

## Conclusions and challenges

The interface bonding status of stainless steel clad plate severely depends on the vacuum degree, rolling temperature and deformation ratio; with the increase in the three fabrication parameters, interfacial shear strength is gradually increased, and the shear fracture region transmits from interface to decarburized layer. The C, Fe, Ni, Cr, Fe diffusion zones are presented at the clad interface. Herein, the diffusion of carbon element leads to the formation of decarburized and carburized layers, which reveals the uphill diffusion and interface concentration. Sufficient diffusion of Cr element results in the improvement of interfacial shear strength. Meanwhile, the addition of Ni interlayer can effectively inhibit the carbon diffusion and improve the interfacial shear strength. Longitudinal tensile fracture characteristics reveal that clad plates with weak interface generate interfacial delamination cracks, resulting in the low fracture elongation of clad plate, whereas clad plates with strong interface can enhance deformation coordination and uniform plastic deformation capacity, which is beneficial for improving the fracture elongation of stainless steel clad plate.

Recently, the investigation and analysis of clad interface of hot-rolled stainless steel clad plate are mainly focused on the macroscale and mesoscale. However, there are few reports relating to the microscale and atom scale. Many reports reveal that the interface bonding properties are mainly related to the interface oxides inclusions containing type, distribution, size, shape and number. Moreover, the distribution state of interface oxides can also affect the alloy element diffusion behavior and macroscale/mesoscale interface transition zone. Actually, the interface oxides inclusions are rather complex, containing more than two alloy elements. Moreover, the interface oxides inclusions are rather fine in microscale, and further investigations and research should be carried out using XPS, FIB, TEM and atom probe. Therefore, more advanced analysis and testing means should be used to reveal the formation, aggregation and evolution process of complex interface oxides inclusions. Meanwhile, laser confocal microscope can be used to investigate the formation and evolution process of clad interface microstructure during the in situ heating process, which may be the further research direction to reveal the bonding mechanism of stainless steel clad plate using in situ technique. In addition, numerical simulation can serve as an effective way to build up the relationship among interface bonding properties, hardness distribution and alloy element diffusion behavior. In this way, the mechanical properties of stainless steel clad plate can be predictable and devisable.

Actually, investigation on interface bonding mechanism of stainless steel clad plate is beneficial to fabricate the large plate with a thick thickness. In general, big casting slabs or large weldments always contain many metallurgical defects during the fabrication process, such as shrinkage cavity, alloy element segregation, excessive inclusions. Therefore, a large hot-rolled plate with strong interface can provide a new design route to avoid the casting defects in the sequence of multiplate encapsulation, welding and hot rolling process. In this way, the tradition design idea "using big casting slab to obtain big sample" can be replaced by "using small casting slab to obtain big sample."

## Acknowledgements

This work is financially supported by the Hebei Province High Education Department High-level Talent Science and Technology Research Project No. GCC2014012, the National Natural Science Foundation of China (NSFC) under Grant Nos. U1860114 and 51601055, the National Natural Science Foundation of Hebei Province under Grant No. E201620218.

## References

[1] Smith L (2012) Engineering with clad steel. Nickel Institute Technical Series, Beijing, pp 1–23

[2] Liu BX, Yin FX, Dai XL, He JN, Fang W, Chen CX, Dong YC (2017) The tensile behaviors and fracture characteristics of stainless steel clad plates with different interfacial status. Mater Sci Eng, A 679:172–182

[3] Song H, Shin H, Shin Y (2016) Heat treatment of clad steel plate for application of hull structure. Ocean Eng 122:278–287

[4] Zhu ZC, He Y, Zhang XJ, Liu HY, Li X (2016) Effect of interface oxides on shear properties of hot-rolled stainless steel clad plate. Mater Sci Eng, A 669:344–349
[5] Fang J, Li YZ (2012) Process optimization for welding stainless steel clad material based on orthotropic bridge plates. Appl Mech Mater 178–181:2066–2069
[6] Miki C, Homma K, Tominaga T (2002) High strength and high performance steels and their use in bridge structure. J Constr Steel Res 58:3–20
[7] Su H, Luo XB, Chai F, Shen JC, Sun XJ, Lu F (2015) Manufacturing technology and application trends of titanium clad steel plates. J Iron Steel Res Int 22:977–982
[8] Ye Y, Zhang SJ, Han LH, Liu Y (2018) Square concrete-filled stainless steel/carbon steel bimetallic tubular stub columns under axial compression. J Constr Steel Res 146:49–62
[9] Marques MJ, Ramasamy A, Batusta AC, Nobre JP, Loureiro A (2015) Effect of heat treatment on microstrucutre and residual stress fields of a weld multilayer austenitic steel clad. J Mater Process Technol 222:52–60
[10] Zhang LJ, Pei Q, Zhang JX, Bi ZY, Li PC (2014) Study on the microstructure and mechanical properties of explosive welded 2205/x65 bimetallic sheet. Mater Des 64:462–476
[11] Mendes R, Ribeiro JB, Loureiro A (2013) Effect of explosive characteristics on the explosive welding of stainless steel to carbon steel in cylindrical configuration. Mater Des 51:182–192
[12] Satya Prasad VV, Madhusudhan Reddy G (2012) Microstructure and mechanical properties of electroslag strip and explosively clad low alloy steel: stainless steel joints. Trans Indian Inst Met 65:135–143
[13] Yazdani M, Toroghinejad MR, Hashemi SM (2016) Effects of heat treatment on interface microstructure and mechanical properties of explosively welded Ck60/St37 plates. J Mater Eng Perform 25:5330–5342
[14] Niederhauser S, Karlsson B (2003) Mechanical properties of laser cladded steel. Mater Sci Technol 19:1611–1616
[15] Pongmorakot K, Nambu S, Koseki T (2018) Effects of compressive strain on the evolution of interfacial strength of steel/nickel solid-state bonding at low temperature. Sci Technol Weld Join 23:344–350
[16] Pongmorakot K, Nambu S, Shibuta Y, Koseki T (2017) Investigation on the mechanism of steel/steel solid-state bonding at low temperatures. Sci Technol Weld Join 22:257–263
[17] Xu W, Sun X (2016) Numerical investigation of electromagnetic pulse welded interfaces between dissimilar metals. Sci Technol Weld Join 21:592–599
[18] Chen KK, Zhang YS, Wang HZ (2017) Study of plastic deformation and interface friction process for ultrasonic welding. Sci Technol Weld Join 22:208–216
[19] Tanaka T, Fukuchi Y (1983) Fatigue crack propagation behavior of two-layered low carbon steel-stainless steel composite plates. Bull JSME 26:1273–1280
[20] Honda K, Torii T (1981) Study on fatigue fracture of laminated inhomogeneous metals (in quenched clad plates of low carbon steel and middle carbon steel). Bull JSME 24:468–474
[21] Wang S, Liu BX, Chen CX, Feng JH, Yin FX (2018) Microstructure, mechanical properties and interface bonding mechanism of hot-rolled stainless steel clad plates at different rolling reduction ratios. J Alloy Compd 766:517–526
[22] Xie GM, Luo ZG, Wang GL, Li L, Wang GD (2011) Interface characteristic and properties of stainless steel/HSLA steel clad plate by vacuum rolling cladding. Mater Trans 52:1709–1712
[23] Li L, Yin FX, Nagai K (2011) Progress of laminated materials and clad steels production. Mater Sci Forum 675–677:439–447
[24] Tachibana S, Koronuma Y, Yokota T, Yamada K, Moriya Y, Kami C (2015) Effect of hot rolling and cooling conditions on intergranular corrosion behavior in alloy625 clad steel. Corros Sci 99:125–133
[25] Li L, Nagai K, Yin FX (2008) Progress in cold roll bonding of metals. Sci Technol Adv Mater 9:1–11
[26] Chen CX, Liu MY, Liu BX, Yin FX, Dong YC, Zhang X, Zhang FY, Zhang YG (2017) Tensile shear sample design and interfacial shear strength of stainless steel clad plate. Fusion Eng Des 125:431–441
[27] Bouaziz O, Masse JP, Petitgand G, Huang MX (2016) A novel strong and ductile TWIP/Martensite steel composite. Adv Eng Mater 18:56–59
[28] Jiang WC, Xu XP, Gong JM, Tu ST (2012) Influence of repair length on residual stress in the repair weld of a clad plate. Nucl Eng Des 246:211–219
[29] Jiang F, Deng ZL, Zhao K, Sun J (2003) Fatigue crack propagation normal to a plasticity mismatched biomaterial interface. Mater Sci Eng, A 356:258–266
[30] Nambu S, Michiuchi M, Inoue J, Koseki T (2009) Effect of interfacial bonding strength on the tensile ductility of multilayered steel composites. Compos Sci Technol 69:1936–1941
[31] Missori S, Murdolo F, Sili A (2004) Single-pass laser beam welding of clad steel plate. Weld J 83:65–71
[32] Dhib Z, Guermazi N, Gasperini M, Haddar N (2016) Cladding of low-carbon steel to austenitic stainless steel by

hot-roll bonding: microstructure and mechanical properties before and after welding. Mater Sci Eng, A 656:130–141

[33] Rees DWA, Power RK (1994) Forming limits in a clad steel. J Mater Process Technol 45:571–575

[34] Li HB, Chen J, Yang J (2013) Experiment and numerical simulation on delamination during the laminated steel sheet forming processes. Int J Adv Manuf Technol 68:641–649

[35] Dhib Z, Guermazi N, Ktari A, Gasperini M, Haddar N (2017) Mechanical bonding properties and interfacial morphologies of austenitic stainless steel clad plates. Mater Sci Eng, A 696:374–386

[36] Atrian A, Fereshteh-Saniee F (2013) Deep drawing process of steel/brass laminated sheets. Compos Part B 47:75–81

[37] Liu BX, Huang LJ, Geng L, Wang B, Cui XP, Liu C, Wang GS (2013) Microstructure and tensile behavior of novel laminated Ti–TiBw/Ti composites by reaction hot pressing. Mater Sci Eng, A 583:182–187

[38] Liu BX, Huang LJ, Kaveendran B, Geng L, Cui XP, Wei SL, Yin FX (2017) Tensile and bending behaviors and characteristics of laminated Ti–(TiBw/Ti) composites with different interface status. Compos B 108:377–385

[39] Liu BX, Huang LJ, Geng L, Wang B, Liu C, Zhang WC (2014) Fabrication and superior of laminated Ti–TiBw/Ti composites by diffusion welding. J Alloy Compd 602:187–192

[40] Kum DW, Oyama T, Wadsworth J, Sherby OD (1983) The impact properties of laminated composites containing ultrahigh carbon (UHC) steels. J Mech Phys Solids 31:173–186

[41] Liu BX, Huang LJ, Rong XD, Geng L, Yin FX (2016) Bending behaviors and fracture characteristics of laminated ductile-tough composites under different modes. Compos Sci Technol 126:94–105

[42] Cepeda-Jiménez CM, Lutfullin RY, Ruano OA (2013) Effect of processing temperature on the texture and shear mechanical properties of diffusion bonded Ti–6Al–4V multilayer laminates. Metall Mater Trans A 44:4743–4753

[43] Liu BX, Wang S, Ma JL, Yin FX, Feng JH, Chen CX (2018) Microstructure and mechanical properties of hot-rolled stainless steel clad plates by heat treatment. Mater Chem Phys 216:460–467

[44] Jing Y, Qin Y, Zang XM, Shang QY, Song H (2014) A novel reduction-bonding process to fabricate stainless steel clad plate. J Alloy Compd 617:688–698

[45] Jing Y, Qin Y, Zang XM, Li YH (2014) The bonding properties and interfacial morphologies of clad plate prepared by multiple passes hot rolling in a protective atmosphere. J Mater Process Technol 214:1686–1695

[46] Madaah-Hosseini HR, Kokabi AH (2002) Cold roll bonding of 5754-aluminum strips. Mater Sci Eng, A 335:186–190

[47] Li L, Zhang XJ, Zhu ZC, Liu HY (2014) Investigation on bonding of stainless steel clad plate by vacuum hot rolling. J Mater Metall 13:46–50 **(in Chinese)**

[48] Mehr VY, Toroghinejad MR, Rezaeian A (2014) The effects of oxide film and annealing treatment on the bond strength of Al–Cu strips in cold roll bonding process. Mater Des 53:174–181

[49] Zhang XJ, Li L, Liu HY, Yin FX (2013) Application of insert layer in manufacturing clad metal plates. Steel Roll 30:45–49 **(in Chinese)**

[50] Jamaati R, Toroghinejad MR (2011) The role of surface preparation parameters on cold roll bonding of aluminum strips. J Mater Eng Perform 20:192–197

[51] Wu HY, Lee S, Wang JY (1998) Solid-state bonding of iron-based alloys, steel–brass, and aluminum alloys. J Mater Process Technol 75:173–179

[52] Jamaati R, Toroghinejad MR (2011) Cold roll bonding bond strengths: review. Mater Sci Technol 27:1101–1108

[53] Wu ZJ, Peng WF, Shu XD (2017) Influence of rolling temperature on interface properties of the cross wedge rolling of 42CrMo/Q235 laminated shaft. Int J Adv Manuf Technol 91:517–526

[54] Li L, Zhang XJ, Liu HY, Yin FX (2013) Formation mechanism of oxide inclusion on the interface of hot-rolled stainless steel clad plates. J Iron Steel Res 25:43–47 **(in Chinese)**

[55] Masahiro N, Ikuro H, Shinji K (2006) Effects of surface oxides on the phospatability of the high strength cold rolled steel. Tetsu Hagane 92:378–384 **(in Japanese)**

[56] Wang GL (2013) Research on interface inclusions' evolution mechanism and process control of vacuum hot roll-cladding. Doctor thesis of Northeastern University, 1–162. (**in Chinese**)

[57] Liu BX, Wang S, Chen CX, Fang W, Yin FX (2019) Interface characteristics and fracture behavior of hot rolled stainless steel clad plates with different vacuum degrees. Appl Surf Sci 463:121–131

[58] Qin Q, Wu ZH, Zang Y, Guan B, Zhang FX (2016) Warping deformation of 316l/Q345r stainless composite plate after removal strake. World J Eng 13:206–209

[59] Qin Q, Zhang DT, Zang Y, Guan B (2015) A simulation study on the multi-pass rolling bond of 316L/Q345R stainless clad plate. Adv Mech Eng 7:1–13

[60] Tong JG, Chen R, Bao WP, Yan K, Ren XP (2009) Composite rolling of three-layer iron-based metals of 25CrMoA steel/micro-alloyed steel/A235 steel. J Univ Sci Technol Beijing 31:186–192 **(in Chinese)**

[61] Jin JB (2013) Research of cladding rate and shear strength for hot rolled stainless steel clad plate. Wide Heavy Plate 19:12–15 **(in Chinese)**

[62] Kolarik L, Janovec J, Kolarikova M, Nachtnebl P (2015) Influence of diffusion welding time on homogenous steel joints. Proc Eng 100:1678–1685

[63] He JY, Ma Y, Yan DS, Jiao SH, Yuan FP, Wu XL (2018) Improving ductility by increasing fraction of interfacial zone in low C steel/304SS laminates. Mater Sci Eng, A 726:288–297

[64] Zhang LJ, He Y, Liu HY, Zhang XJ, Liu BL (2016) Effect of induction heating on carbon steel layer in stainless steel clad plates. CFHI Technol 171:52–56 **(in Chinese)**

[65] Li L, Zhu ZC, Zhang XJ, Liu HY (2015) Experimental study on hot rolled stainless steel clad plate produced by TMCP. J Mater Eng 43:62–67 **(in Chinese)**

[66] Motarjemi AK, Kocak M, Ventzke V (2002) Mechanical and fracture characterization of a bi-material steel plate. Int J Press Vessel Pip 79:181–191

[67] Hedayati O, Korei N, Adeli M, Etminanbakhsh M (2017) Microstructural evolution and interfacial diffusion during heat treatment of hastelloy/stainless steel bimetals. J Alloy Compd 712:172–178

[68] Rajeev R, Samajdar I, Raman R, Harendranath CS, Kale GB (2001) Origin of hard and soft zone formation during cladding of austenitic/duplex stainless steel on plain carbon steel. Mater Sci Technol 17:1005–1010

[69] Ayer R, Mueller RR, Leta DP, Sisak WJ (1989) Phase transformations at steel/in625 clad interfaces. Metall Trans A 20:665–681

[70] Pavlovsky J, Million B, Ciha K, Stransky K (1991) Carbon redistribution between an austenitic cladding and a ferritic steel for pressure vessels of nuclear reactor. Mater Sci Eng, A 149:105–110

[71] Mas F, Tassin C, Valle N, Robaut F, Charlot F, Yescas M, Roch F, Todeschini P, Brechet Y (2016) Metallurgical characterization of coupled carbon diffusion and precipitation in dissimilar steel welds. J Mater Sci 51:4846–4879. https://doi.org/10.1007/s10853-016-9792-z

[72] Li L, Zhang XJ, Liu G, Fu HY, Li MN (2015) Effect of Ni layer thickness on bonding strength of hot rolled clad steel plate. Trans Mater Heat Treat 36:80–85

[73] Luo ZA, Wang GL, Xie GM (2013) Interfacial microstructure and properties of a vacuum hot roll bonded titanium stainless steel clad plate with a niobium interlayer. Acta Metall Sin 26:754–760

[74] Pozuelo M, Carreno F, Carsi M, Ruano OA (2007) Influence of interfaces on the mechanical properties of ultrahigh carbon steel multilayer laminates. Int J Mat Res 98:47–52

[75] Syn CK, Lesuer DR, Wolfenstine J, Sherby OD (1993) Layer thickness effect on ductile tensile fracture of ultra-high carbon steel–brass laminates. Metall Trans A 24:1647–1653

[76] Liang F, Tan HF, Zhang B, Zhang GP (2017) Maximizing necking-delayed fracture of sandwich-structured Ni/Cu/Ni composites. Scr Mater 134:28–32

[77] Liu HS, Zhang B, Zhang GP (2011) Delaying premature local necking of high strength Cu: a potential way to enhance plasticity. Scr Mater 64:13–16

[78] Tan HF, Zhang B, Kang YK, Zhu XF, Zhang GP (2016) Fracture behavior of sandwich-structured metal/amorphous alloy/metal composites. Mater Des 90:60–65

[79] Park J, Kim JS, Kang MJ, Sohn SS, Cho WT, Kim HS, Lee S (2017) Tensile property improvement of TWIP-cored three layer steel sheets fabricated by hot roll bonding with low carbon steel or interstitial free steel. Sci Rep 7:40231

[80] Serror MH (2013) Analytical study for deformability of laminated sheet metal. J Adv Res 4:83–92

[81] Guo X, Weng GJ, Soh AK (2012) Ductility enhancement of layered stainless steel with nanograined interface layers. Comput Mater Sci 55:350–355

[82] Pommier H, Busso EP, Morgeneyer TF, Pineau A (2016) Intergranular damage during stress relaxation in AISI 316L-type austenitic stainless steels: effect of carbon, nitrogen and phosphorus. Acta Mater 103:893–908

[83] Jones R, Randle V, Owen G (2008) Carbide precipitation and grain boundary plane selection in overaged type 316 austenitic stainless steel. Mater Sci Eng, A 496:256–261

[84] Sun GS, Du LX, Hu J, Xie H, Wu HY, Misra RDK (2015) Ultrahigh strength nano/ultrafine-grained 304 stainless steel through three-stage cold rolling and annealing treatment. Mater Charact 110:228–235

[85] Avramovic-Cingara G, Ososkov Y, Jain MK, Wilkinson DS (2009) Effect of martensite distribution on damage behavior in DP600 dual phase steels. Mater Sci Eng, A 516:7–16

[86] Eskandari M, Kermanpur A, Najafizadeh A (2009) Formation of nanocrystalline structure in 301 stainless steel produced by martensite treatment. Metall Mater Trans A 40:2241–2249

[87] Eskandari M, Kermanpur A, Najafizadeh A (2009) Formation of nano-grained structure in a 301 stainless steel using a repetitive thermo-mechanical treatment. Mater Lett 63:1442–1444

[88] Bowden EP, Tabor D (1939) The area of contact between stationary and between moving surfaces. Proc R Soc Lond A 169:391–413

[89] Burton MS (1954) Metallurgical principles of metal bonding. Weld J 33:1051–1057

[90] Cave JA, Williams JD (1973) The mechanism of cold pressure welding by rolling. J Inst Met 101:203–207
[91] Derby B, Wallach ER (1984) Diffusion bonding: development of theoretical model. Mater Sci 18:427–431
[92] Mitani Y, Vargas R, Zavala M (1984) Deformation and diffusion bonding of aluminide-coated steels. Thin Solid Films 111:37–42
[93] Brown DW, Okuniewski MA, Sisneros TA, Clausen B, Moore GA, Balogh L (2016) Neutron diffraction measurement of residual stresses, dislocation density and texture in Zr-bonded U-10Mo "mini" fuel foils and plates. J Nucl Mater 482:63–74
[94] Pan D, Gao K, Yu J (1989) Cold roll bonding of bimetallic sheets and strips. Mater Sci Technol 5:934–939
[95] Shirzadi AA, Assadi H, Wallach ER (2001) Interface evolution and bond strength when diffusion bonding materials with stable oxide films. Surf Interface Anal 31:609–618
[96] Parks JM (1953) Recrystallization in welding. Weld J Suppl 32:209–222
[97] Barabash RI, Barabash OM, Ojima M, Yu ZZ, Inoue J, Nambu S, Koseki T, Xu RQ, Feng ZL (2014) Interphase strain gradients in multilayered steel composite from microdiffraction. Metall Mater Trans A 45:98–108
[98] Min XH, Emura S, Meng FQ, Mi GB, Tsuchiya K (2015) Mechanical twinning and dislocation slip multilayered deformation microstructures in $\beta$-type Ti–Mo base alloy. Scr Mater 102:79–82
[99] Bay N (1979) Cold pressure welding-the mechanisms governing bonding. J Eng Ind 101:122–127
[100] Bay N (1983) Mechanisms producing metallic bonds in cold welding. Weld Res Suppl 5:137–142
[101] Zhang W, Bay N (1997) Cold welding-theoretical modeling of the weld formation. Weld Res Suppl 10:417–430
[102] Bay N, Bjerregaard H, Petersen SB (1994) Cross shear roll bonding. J Mater Process Technol 45:1–6
[103] Tylecote RF, Howd D, Furmidage JR (1958) The influence of surface films on the pressure welding of metals. Br Weld J 5:21–38
[104] Milner DR, Rowe GW (1962) Fundamentals of solid-phase welding. Metall Rev 7:433–480
[105] Zhang W, Bay N (1997) A numerical model for cold welding of metals. CIRP Ann 46:195–200
[106] Wang GL, Zuo ZA, Xie GM (2011) Experiment research on impact of total rolling reduction ratio on the properties of vacuum rolling bonding ultra-thick steel plate. Adv Mater Res 299–300:962–965
[107] Suehiro M, Hashimoto Y (1989) Carbon distribution near interface between base and cladding steels in austenite stainless clad steel sheet. Tetsu Hagane 75:1501–1507
[108] Kurt B, Calik A (2009) Interface structure of diffusion bonded duplex stainless steel and medium carbon steel couple. Mater Charact 60:1035–1040
[109] Huang ML, Wang L (1998) Carbon migration in 5Cr–0.5Mo/21Cr–12Ni dissimilar metal clad. Metall Mater Trans A 29:3037–3046
[110] Sawanishi C, Ogura T, Sumi H, Oi K, Yasuda K, Hirose A (2012) Interfacial microstructure observation and nanoindentation measurements in mild steel/HT780 clad plate. Mater Sci Technol 28:1459–1464
[111] Gomez X, Echeberria J (2000) Microstructure and mechanical properties of low alloy steel T11-austenitic steel 347H bimetallic tubes. Mater Sci Technol 16:187–193
[112] Liu BX, Wang S, Fang W, Yin FX, Chen CX (2019) Meso and microscale clad interface characteristics of hot-rolled stainless steel clad plate. Mater Charact 148:17–25
[113] Qin YF, He JN, Yin FX, Liu BX, Zhang FY (2017) Effect of Ti particle size on mechanical and tribological properties of TiCN coatings prepared by reactive plasma spraying. Ceram Int 43:16548–16554
[114] Qin YF, He JN, Yin FX, Zhang FY, Liu BX (2017) Influence of initial Ti particle size on microstructure and fracture toughness of reactive plasma sprayed TiCN coatings. Surf Coat Technol 325:482–489
[115] Zhang FY, Li C, Yan MF, He JN, Yang YG, Yin FX (2017) Microstructure and nanomechanical properties of co-deposited Ti–Cr films prepared by magnetron sputtering. Surf Coat Technol 325:636–642
[116] Jamaati R, Toroghinejad MR, Amirkhanlou S, Edris H (2015) Strengthening mechanisms in nanostructured interstitial free steel deformed to high strain. Mater Sci Eng, A 639:656–662
[117] Jamaati R, Toroghinejad MR, Amirkhanlou S, Edris H (2015) Microstructural evolution of nanostructured steel-based composite fabricated by accumulative roll bonding. Mater Sci Eng, A 639:298–306
[118] Jamaati R, Toroghinejad MR, Edris H, Salmani MR (2014) Fracture of steel nanocomposite made using accumulative roll bonding. Mater Sci Technol 30:1973–1982
[119] Moradgholi J, Monshi A, Farmanesh K, Toroghinejad MR, Loghman-Estarki MR (2017) Comparison of microstructure, toughness, mechanical properties and work hardening of titanium/$TiO_2$ and titanium/SiC composites manufactured by accumulative roll bonding (ARB) process. Ceram Int 43:7701–7709
[120] Takeuchi T, Kakubo Y, Matsukawa Y, Nozawa Y, Toyama T, Nagai Y, Nishiyama Y, Katsuyama J, Yamaguchi Y, Onizawa K, Suzuki M (2014) Effect of thermal aging on microstructure and hardness of stainless steel weld-overlay

claddings of nuclear reactor pressure vessels. J Nucl Mater 452:235–240

[121] Rashid RA, Abaspour S, Palanisamy S, Matthews N, Dargusch MS (2017) Metallurgical and geometrical characterization of the 316L stainless steel clad deposited on a mild steel substrate. Surf Coat Technol 327:174–184

[122] Rao NV, Sarma DS, Nagarjuna S, Reddy GM (2009) Influence of hot rolling and heat treatment on structure and properties of HSLA steel explosively clad with austenitic steel. Mater Sci Technol 25:1387–1396

[123] Liu BX, Huang LJ, Geng L, Wang B, Cui XP (2014) Fracture behaviors and microstructural failure mechanisms of laminated Ti–TiBw/Ti composites. Mater Sci Eng, A 611:290–297

[124] Guo YJ, Qiao GJ, Jian WZ, Zhi XH (2010) Microstructure and tensile behavior of Cu–Al multilayered composites prepared by plasma activated sintering. Mater Sci Eng, A 527:5234–5240

[125] Li T, Suo Z (2006) Deformability of thin metal films on elastomer substrates. Int J Solids Struct 43:2351–2363

[126] Li T, Suo Z (2007) Ductility of thin metal films on polymer substrates modulated by interfacial adhesion. Int J Solids Struct 44:1696–1705

[127] Hsia KJ, Suo Z, Yang W (1994) Cleavage due to dislocation confinement in layered materials. J Mech Phys Solids 42:877–896

[128] Koseki T, Inoue J, Nambu S (2014) Development of multilayer steels for improved combinations of high strength and high ductility. Mater Trans 55:227–237

[129] Inoue J, Nambu S, Ishimoto Y, Koseki T (2008) Fracture elongation of brittle/ductile multilayered steel composites with a strong interface. Scr Mater 59:1055–1058

[130] Hwu KL, Derby B (1999) Fracture of metal/ceramic laminates-I. transition from single to multiple cracking. Acta Mater 47:529–543

[131] Seok MY, Lee JA, Lee DH, Ramamurty U, Nambu S, Koseki T, Jang J (2016) Decoupling the contributions of constituent layers to the strength and ductility of a multilayered steel. Acta Mater 121:164–172

[132] Lesuer DR, Syn CK, Sherby OD, Wadsworth J, Lewandowski JJ, Hunt WH (1996) Mechanical behavior of laminated metal composites. Int Mater Rev 41:169–197

[133] Snyder BC, Wadsworth J, Sherby OD (1984) Superplastic behavior in ferrous laminated composites. Acta Mater 32:919–932

[134] Cohades A, Mortensen A (2014) Tensile elongation of unidirectional or laminated composites combining a brittle reinforcement with a ductile strain and strain-rate hardening matrix. Acta Mater 71:31–43

[135] Cao WQ, Zhang MD, Huang CX, Xiao SY, Dong H, Weng YQ (2016) Ultrahigh charpy impact toughness ($\sim$ 450 J) achieved in high strength ferrite/martensite laminated steels. Sci Rep 7:41459

[136] Pozuelo M, Carreno F, Ruano OA (2006) Delamination effect on the impact toughness of an ultrahigh carbon-mild steel laminate composite. Compos Sci Technol 66:2671–2676

[137] Kimura Y, Inoue T, Yin FX, Tsuzaki K (2008) Inverse temperature dependence of toughness in an ultrafine grain-structure steel. Science 320:1057–1060

[138] Huang LJ, Geng L, Peng HX (2015) Microstructurally inhomogeneous composites: is a homogeneous reinforcement distribution optimal? Prog Mater Sci 71:93–168

[139] Song F, Bai YL (2003) Effects of nanostructures on the fracture strength of the interfaces in nacre. J Mater Res 18:1741–1744

[140] Price RD, Jiang FC, Kulin RM, Vecchio KS (2011) Effects of ductile phase volume fraction on the mechanical properties of Ti–$TiAl_3$ metal-intermetallic laminate (MIL) composites. Mater Sci Eng, A 528:3134–3146

[141] Jackson AP, Vincent JF (1989) A physical model of nacre. Compos Sci Technol 36:255–266

[142] Koyama M, Zhang Z, Wang MM, Ponge D, Raabe D, Tsuzaki K, Noguchi H, Tasan CC (2017) Bone-like crack resistance in hierarchical metastable nanolaminate steel. Science 355:1055–1057